

INFLUENCE OF PART MICROSTRUCTURE ON MECHANICAL PROPERTIES OF PA6X LASER SINTERED SPECIMENS

C. Kummert*, W. Diekmann†, K. Tews* and H.J. Schmid *

*Direct Manufacturing Research Center/ Particle Technology Group, Paderborn University, Paderborn,
Germany

†Evonik Resource Efficiency GmbH, Marl, Germany

Abstract

The influence of different process parameters on mechanical properties of selectively laser sintered (SLS) parts was investigated in various studies. Until now, the significant differences in mechanical characteristics depending on processing conditions are insufficiently explained but reasons may be found in part microstructure. For this reason, PA6x test specimens with different component properties were printed by changing laser exposure strategies and their microstructure was examined using for example XCT-analysis. PA6x is a comparatively new SLS material which offers outstanding mechanical properties if adequate SLS processing parameters are used. In this study different SLS machines are used by EVONIK and the DMRC, Paderborn University to investigate the relationship between SLS-specific manufacturing conditions, the resulting components microstructure and finally the component properties. The knowledge gained can contribute to a deeper understanding of the process.

Introduction

Selective laser sintering is a promising additive manufacturing process for serial production because of its high productivity due to the 3-dimensional set up of the components inside the build space. Besides efficiency, high quality and reproducible build parts are required in the industry. Especially new SLS materials, developed to address the demands of the industry covered with PA12, bring new challenges and have not yet been investigated extensively. When a new material for the SLS process is launched on the market, suitable process parameters must be developed first to generate the best possible characteristic values. Not only optimization of build part properties but also improvement of robustness and homogeneity independent of build orientation, positioning or other process specific effects take place in parameter development. The most controllable parameter in the process is the laser exposure pattern. The influence of the different variables of the laser energy input like laser power and scan speed on resulting part characteristics has been investigated in different works [5, 7].


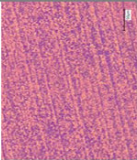

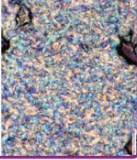
However, mechanical properties are the result of the part microstructure like porosity, crystallinity, state of the polymer chains and the surface structure. These are also influenced by the original powder properties, such as particle size distribution and crystallization temperature and melt degree [4]. Furthermore, the rheological behavior of the polymers is directly related to the degree of particle melt [2, 6]. A higher melt viscosity requires more laser energy input to melt and coalesce the polymer particles. On the other side, insufficient laser energy leads to higher porosity and therefore reduced mechanical properties [7].

Wegner et al. [8] placed greater attention on the latter. They showed that a double laser exposure strategy can help to improve elongation at break and to reduce fluctuations due to cycle time as well as build direction and positioning. As long as the energy input is not too high a second exposure reduces pores and thus improves layer bonding.

A double exposure of the contour region was already found to generate lower porosity within the part edges and therefore to improve mechanical properties especially in z-build direction [3]. Consequently, it would be interesting to know, if there is a maximum porosity inside of the sample which is not compromising part quality provided by the contour has a dense structure. Furthermore, during parameter development for PA613 it could be noticed that despite identical process conditions and parameters elongation at break shows high fluctuations which was already recognized for other materials [6, 8].

When comparing data of injection molded and laser sintered nylon 613 (polyamide 613, PA613) a discrepancy can be noticed (see Table 1). As already known from PA12 PA613 shows also a shift to a slightly higher young's modulus from about 1900 MPa (molded) to 2000 MPa (printed). Also known from PA12 is that the tensile strength of injection molded and laser sintered parts is comparable. This is also the case for PA613 which shows a tensile strength of about 55 MPa. The mentioned discrepancy can be found in elongation at break (EaB) and notched impact strength (NIS). While injection molded PA12 has a higher EaB and NIS than injection molded PA613, the opposite can be observed after laser sintering both nylons, i.e. PA613 now shows a higher EaB and NIS than PA12.

Table 1: Data for injection molded and laser sintered parts of PA12 and PA613

Material & Process	Test method	Tensile Testing			Charpy test	Density Archimedes	Microscopy
	Property	Youngs modulus	Tensile strength	Elongation at Break	Notched impact strength at RT	Density	crystallinity
	Unit	MPa	MPa	%	KJ/m²	g/cm³	---
PA12 PA6x Injection molding		1500	45	>300	35	1,01	
		1900	55	>200	7	1,055	
PA12 PA6x Laser sintering		1650	45	15	3	0,95-1,00	
		2000	55	40	5	1,00-1,05	

Data were generated by building parts with special parameters. The mechanical properties can e.g. vary depending on the part position (SLS), type of test bar and the operating conditions which are used. Injection molded specimen are made with standard settings. Elaborated settings can lead to different results.

In order to better understand these effects, the microstructure shall be examined more closely. Porosity, crystallinity and crystalline structure are known to have a high influence on mechanical properties [1, 4]. With increasing crystallinity and ordered lamella in spherulites part strength is pronounced. On the other hand side, elasticity requires amorphous regions [1]. To take these microstructural properties into account crystallinity is measured by DSC (differential scanning calorimetry) and spherulites are detected with light microscopy.

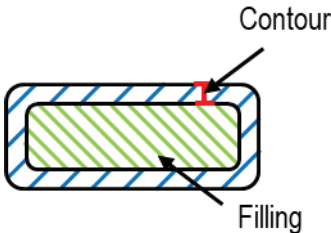


Figure 1: Cross section of tensile specimen

In the following, laser exposure parameters of the filling and contour (see Figure 1) are varied on two different SLS machine types to build PA613 specimens. Microstructural properties, especially the porosity are correlated with mechanical properties to find the origin of the sensitivity towards process parameters. In this way, the goal of manufacturing parts with high quality and high reproducibility may be achieved.

The material under investigation is PA613, a high-temperature polyamide with excellent mechanical properties and slightly higher melt temperature developed by Evonik particularly for the laser sintering process. As presented in Table 1 the material VESTOSINT® 3D 8754 HT1 can reach an elongation at break of 40 % in x-build direction applying adequate process parameters. In this work it is used in two different formulations, VESTOSINT® Z2837 showing higher recyclability and VESTOSINT® 3D 8754 HT1 showing the presented higher mechanical properties.

At the DMRC, Paderborn University the material VESTOSINT® Z2837(refresh rate 50/50) is processed on an EOSINT P396 to build z-direction tensile specimens type 1A (DIN EN 527) for the first two sample series Throughout all experiments the layer thickness was kept constant at 120 µm. Within the first sample series contour parameters are varied in five different ways (C1-C5), whereas the filling parameters (F0) are kept constant. Not only laser power, scan speed and the beam offset are modified but also the sequence of the exposure. This way the influence of the energy input into the contour is evaluated. A second sample series consists of a filling parameter variation and the contour is either C1 or C3 in order to provoke porosity inside of the samples with a dense contour region. Deviating from F0 pores are generated by a higher hatch distance and a lower energy input to reduce the polymer particle coalescence or by a very intense exposure resulting in material evaporation. The corresponding design of experiment is shown in Table 2 and Table 3.

Table 2: Contour exposure parameters of the 1st sample series with VESTOSINT® Z2837

No.	Laser power [W]	Scan speed [mm/s]	Beam offset [mm]	Sequence
C1F0	25	6000	0.35	1x afterwards
C2F0	40	6000	0.225	1x first 1x afterwards
C3F0	40	4500	0.225	2x afterwards
C4F0	40	3000	0.35	2x first
C5F0	40	3000	0.1	2x first

At least four specimens for each parameter set are taken for tensile tests, performed on an INSTRON 5569 EH universal testing machine. The fifth specimen is taken for microstructural tests. Melt enthalpy corresponds to the crystallinity in the following and is determined by DSC (differential scanning calorimetry) measurements. For this purpose a Netzsch DSC 214 Polyma is used with a heating rate of 10 K/min. The XCT-scan (computed X-ray tomography) was performed with GE Phoenix Nanotom S with 70 kV 150 µA and 1440 projections. Furthermore, the 3D XCT-data are analyzed using the “Detect Analysis” of the software VGStudio MAX 2.2 from Volume Graphics GmbH. The algorithm compares the gray scale value with a threshold, so that only defined defect sizes are taken into account. Hereby the voxel size is 10 µm. Furthermore, the Region-Of-Interest (ROI), which is analyzed in detail, was separated into the contour area and filling area as described in [3]. To determine the build part density the immersed body method according to DIN EN ISO 1183 is applied as no uniform dimensions are needed. Therefore, samples are taken of the measuring length and immersed in ethanol. With the help of an analytical balance the weight is determined in air and ethanol. Under consideration of the particular medium densities, part density is calculated.

Table 3: Filling exposure parameters of the 2nd sample series with VESTOSINT® Z2837

No.	Laser power [W]	ScanSpeed [mm/s]	Hatch distance [mm]
C1F1	15	6000	0.16
C1F2	15	6000	0.3
C1F3	25	6000	0.16
C1F4	25	6000	0.3
C3F1	15	6000	0.16
C3F2	15	6000	0.3
C3F5	40	4500	0.16
C3F6	40	4500	0.3
F0	25	4750	0.16

VESTOSINT 3D 8754 HT1 was also printed on an EOSINT P395 at Evonik. The layer thickness was always 100 µm and six different sets of parameters (see Table 4) were used to determine the influence on part properties. Especially differences in crystallinity and crystal structure were focussed. To analyse crystallinity DSC and to investigate part structure light microscopy were used.

Table 4: Parameters used at Evonik with VESTOSINT 3D 8754 HT1

No.	Hatch	Filling Energy density [J/cm³]	Contour sequence	Contour Laser power [W]	Contour Scan Speed [mm/s]
E1	1x	575	1x first	14	700
E2	1x	575	1x first, 1x afterwards	14	700
E3	1x	455	1x afterwards	14	700
E4	1x	665	1x afterwards	14	700
E5	1x	390	1x afterwards	14	700
E6	1x	575	1x afterwards	14	700

Results and Discussions

The following diagrams show the results of tensile tests and the microstructural investigations. For the first sample series the focus was the variation of contour exposure parameters to evaluate their effect on mechanical properties. Figure 2 shows tensile strength, elongation at break and the contour porosity for the different parameters. While quite low contour porosity of C2F0 and C3F0 results in high mechanical values, a very high contour porosity detected for sample numbers C5F0 and C4F0 causes very poor elongation at break. On the other hand, omitting extra contour exposure completely (F0) leads to acceptable tensile properties. The high contour porosity of C5F0 has its origin in the quite high energy input of the contour parameters of C5 which leads to a porous ring and therefore to premature material failure. The porous ring of C5F0 gets visible in Figure 3 and is already discussed in [3]. Also, C4F0 shows more pores in the contour region in comparison to example C1F0.

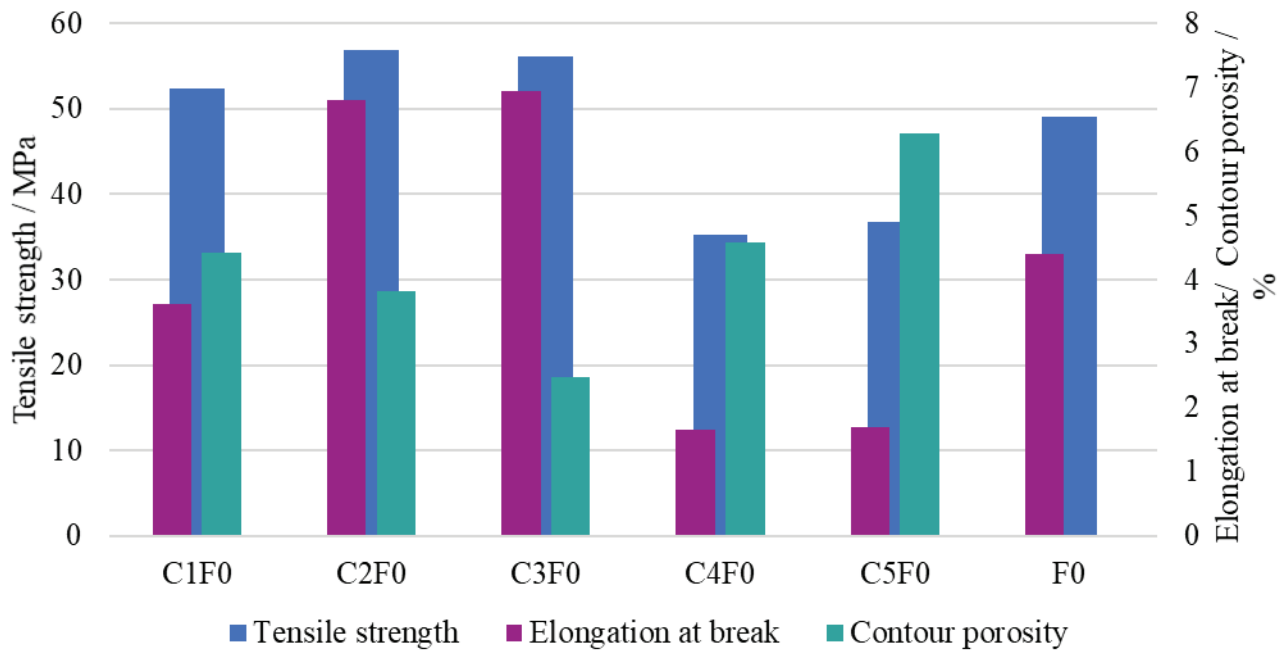


Figure 2: Tensile properties and contour porosity of the first sample row

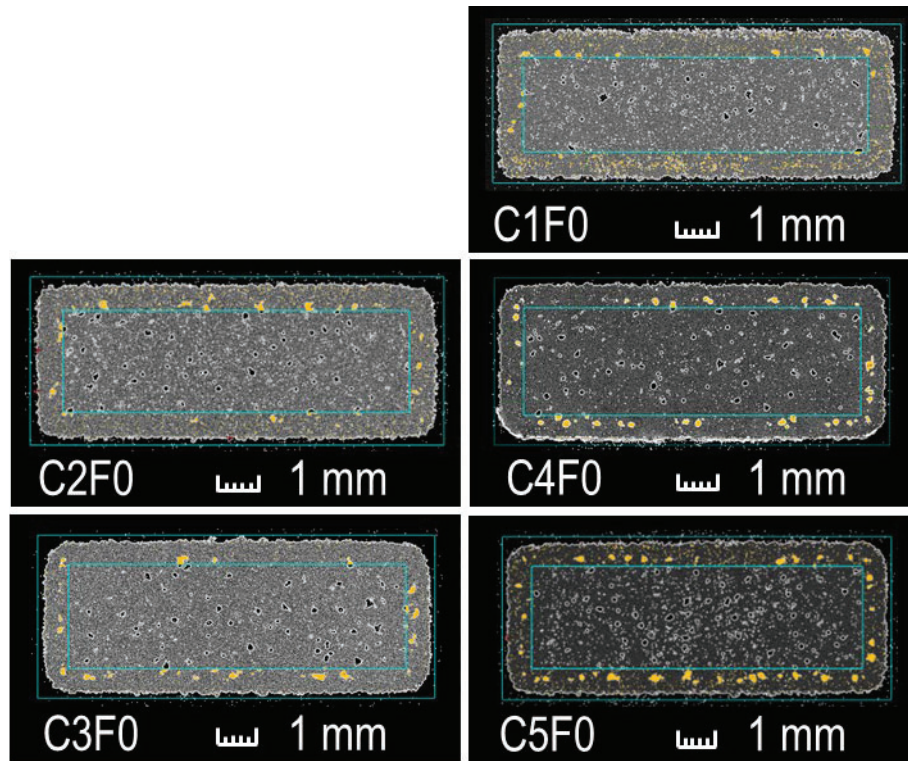


Figure 3: XCT-scan pictures of tensile specimens cross sections of the 1st sample row

Within the second sample series the filling exposure parameters are varied, so that the porosity inside of the sample is depicted together with the mechanical properties in Figure 5. High porosity could be generated for example inside of the samples C1F2 and C3F2. The contour exposure parameters C1 and C3 which led in sample row 1 to an improvement of the mechanical characteristic generate actually a dense contour region which is visible in Figure 4 but could not compensate the high number of defects inside of the samples. Nevertheless, samples built with contour parameters C3 on average show higher mechanical properties, while the filling porosity is not clearly lower in comparison to the ones of C1. Comparison of C3F6 with F0 shows quite similar elongation at break and tensile strength although the porosity of F0 is higher. C3F5 results as well in a high elongation at break while the filling porosity is comparatively poor. Here, neither contour exposure nor porosity seem to be the determining factors.

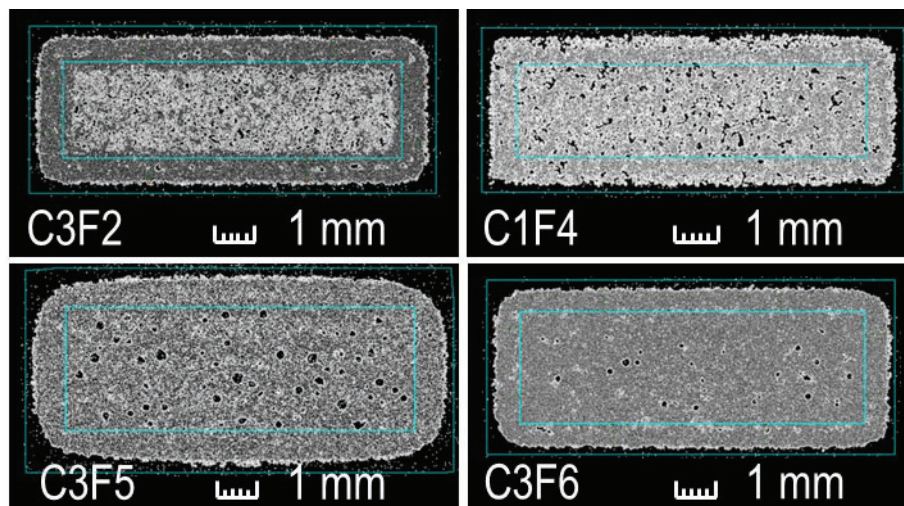


Figure 4: XCT-scan pictures of tensile specimen cross sections of the 2nd sample row

Furthermore, contour and filling exposure seem mutually interact concerning the total energy input. Regarding C3F5 and C3F6 contour exposure parameters are indeed the same but pictures in Figure 4 show that C3F5 has more big pores in the core and furthermore that the cross section is enlarged. The energy input by F5 might be that high, that material is melted on beyond the contour region and the observed pore development inside of the sample might be accounted to material degradation. Nevertheless, the contour is quite dense with a porosity of 3.57 % and mechanical characteristics are still not decreased. On the contrary C1F4 shows only slightly higher filling porosity but a more porous contour region which results in reduced mechanical properties. Viewing the XCT-pictures in Figure 4 reveals further that the shape of the pores are different from the ones of C3F5. Here incomplete particle coalescence due to insufficient laser energy input seems to be the reason for the pore development. With increasing total energy input the coalescence of polymer particles is favored and therefore porosity reduced.

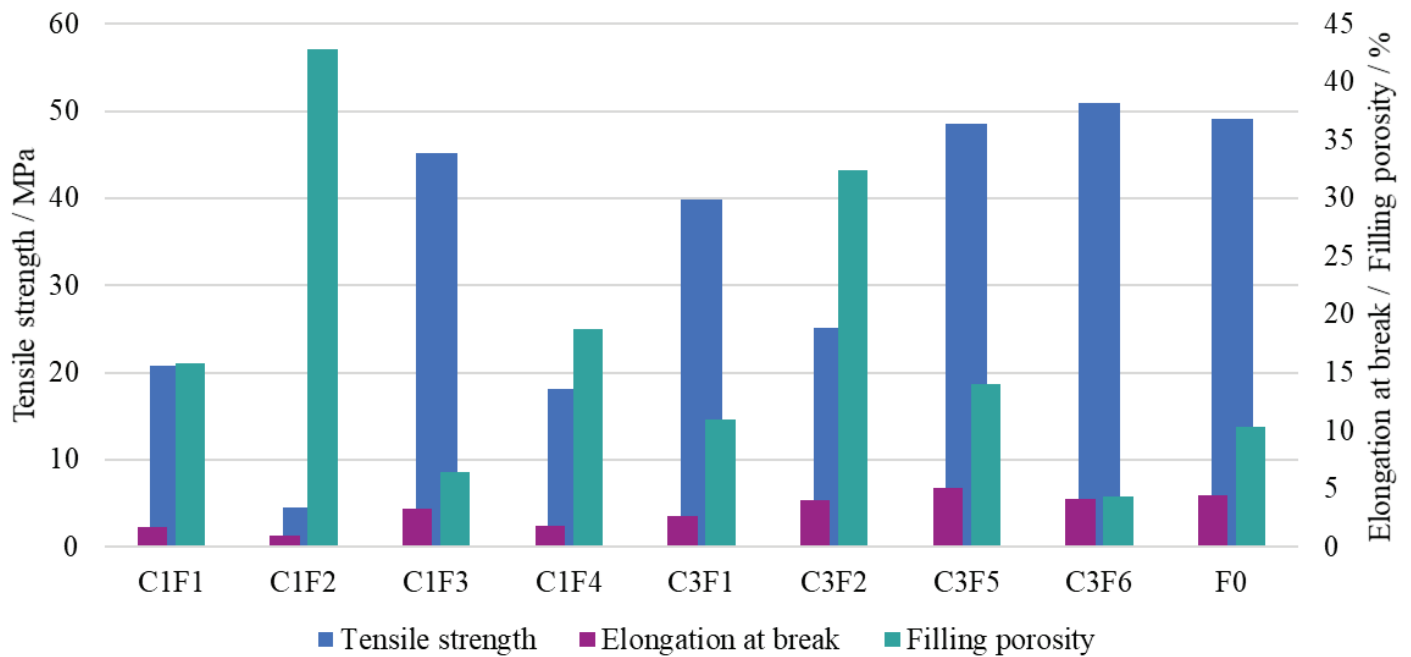


Figure 5: Tensile properties and filling porosity of the second sample row

The porosity of both sample series are directly reflected in measured part densities. In Figure 6 the filling porosity evaluated from the XCT-scans and sample density which was measured by immersed body method is depicted for both sample rows. As to be expected, density is low when the filling porosity is high and vice versa. Furthermore, the constant filling exposure parameters of the 1st sample series indeed result in a quite constant high part density.

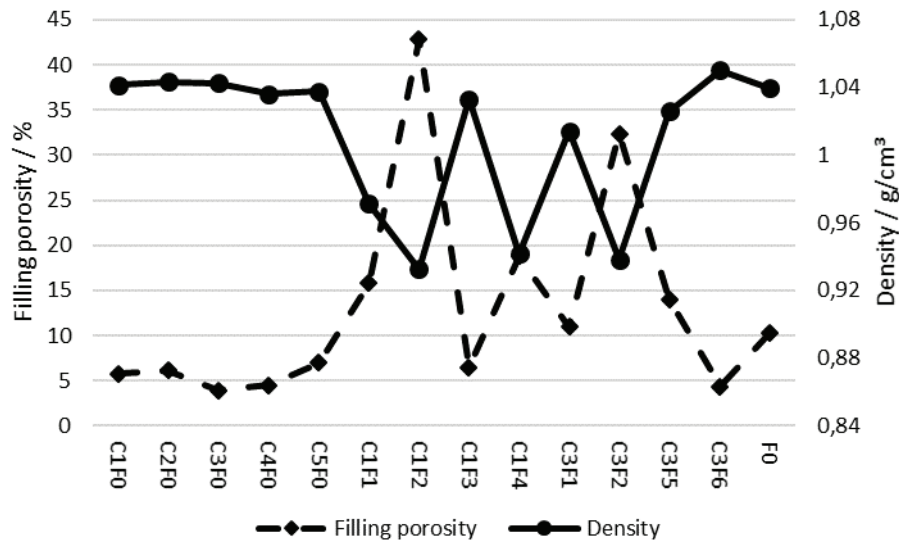


Figure 6: Comparison of filling porosity and sample density of the 1st and 2nd sample row

Figure 7 shows that at low densities the mechanical properties are strongly depending on part density. However, if a given density around 1 g/cm³ is reached, mechanical properties are only weakly sensitive to porosity / density any more. The figure shows not only densities and mechanical properties of samples from the DMRC but also of the ones manufactured and tested at Evonik with a different material VESTOSINT® 3D 8754 HT1 which is not recyclable. The quite low tensile strength at a high density of 1.038 g/cm³ is the result of the high contour porosity of C5F0. However, the strong scattering of mechanical properties even for similar filling porosity indicate, that there is origin, most probably in other microstructural properties.

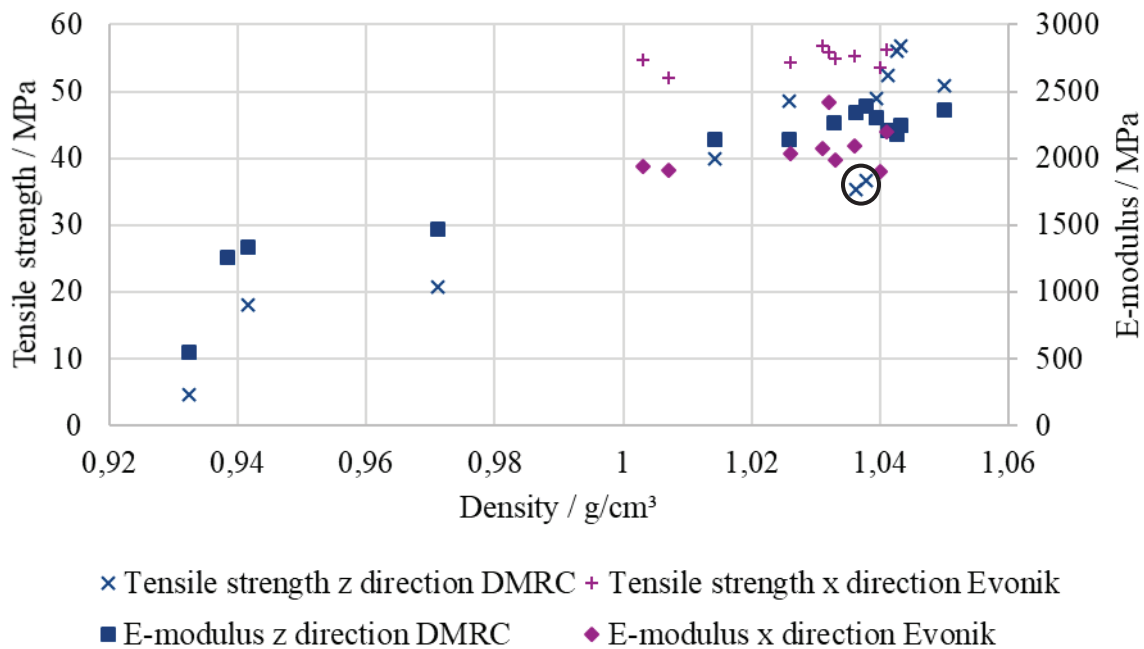
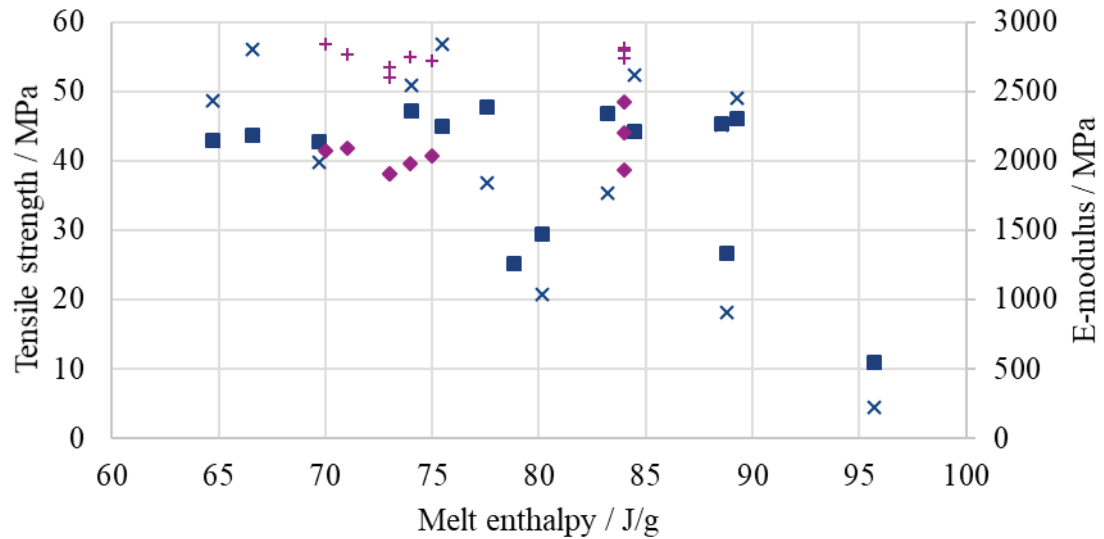


Figure 7: Part density in correlation to mechanical properties

For this reason, tensile properties of all sample series are shown with respect to melt enthalpy as an indication for crystallinity in Figure 8. Apart from the very low mechanical properties at a high melt enthalpy of 95 J/g, no significant tendency is detectable. Here, porosity seem to be more crucial and to mask possible influences of the crystallinity on mechanical properties.



× Tensile strength z direction DMRC + Tensile strength x direction Evonik
 ■ E-modulus z direction DMRC ◆ E-modulus x direction Evonik

Figure 8: Melt enthalpy in correlation to mechanical properties

The analysis of injection molded and printed specimens (Figure 9) of PA12 and PA613 by light spectroscopy illustrates the differences in crystal structure. While injection molded parts show small, equally distributed crystals in the middle and a less crystalline, more amorphous shell for both materials (PA12 and PA613), big differences in laser sintered parts are visible. For PA12, the difference in crystallinity is expected and known, but PA613 shows, besides typical layers and bubbles of laser sintering processes, also amorphous sections. This is a significant difference to the high crystallinity and “big” spherulites of PA12. Some of the parts made out of PA613 show significant higher values with respect to elongation at break. Analysed tensile bars with outstanding 80 % elongation at break show less spherulites than tensile bars that reached 30 % elongation. The study is continued and so far, there is no proof that crystal structure and properties correlate.

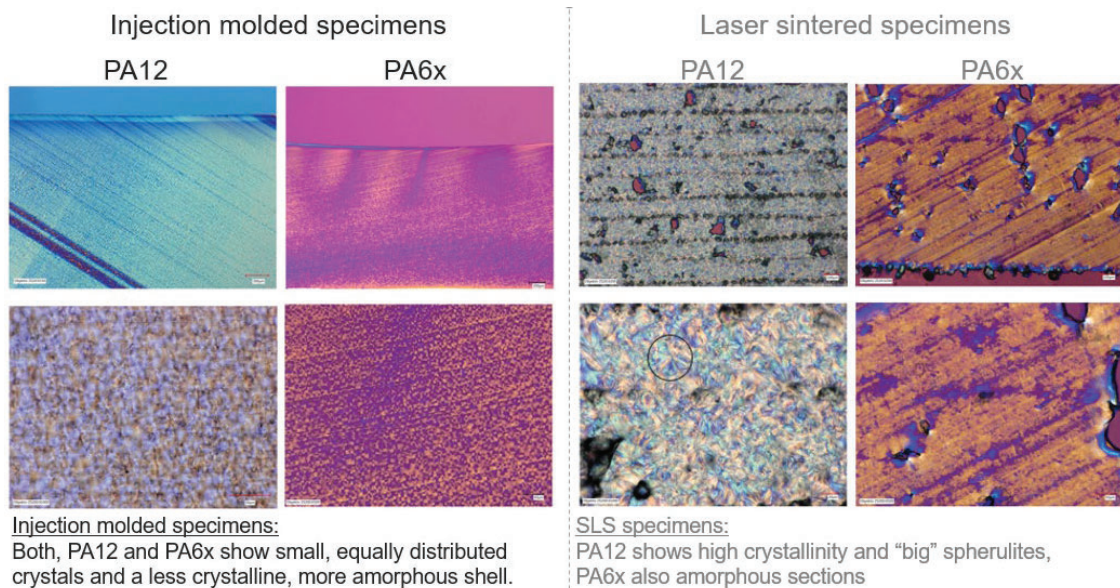


Figure 9: Light spectroscopy images of injection molded and laser sintering specimens

Conclusion and outlook

In this work, different laser parameter variations of the contour and filling strategy have been performed with to different materials at the DMRC and at Evonik to investigate the correlation between PA613 specimen's microstructure and corresponding mechanical properties. Besides porosity analysis, density and crystallinity have been tested to find the dominating reason for component failure. It becomes obvious, that density measurement reproduces porosity results of XCT-scans pretty well. Further, it could be shown that provoked porosity inside of the sample and a porous ring in the contour region as well lead to reduced tensile properties. Nevertheless, when a certain degree of density is reached, neither porosity nor crystallinity seem to be decisive. As the influence of crystallinity might be overlapped by the high provoked porosity and first considerations of spherulites were promising further investigations are planned. By a variation of exposure parameters resulting all in dense samples the effect of crystallinity shall be evaluated whereas porosity is avoided in the future. Further origins of fluctuations especially of elongation at break might be crystallite size, polymer chain length and surface defects which will also be regarded.

Overall, the PA6 like material is more sensitive to process parameters in comparison to standard LS material PA12 but can get also closer to injection molded PA6 properties when using suitable settings.

References

- [1] Kantesh Balani, Vivek Verma, Arvind Agarwal, and Roger Narayan. Physical, Thermal, and Mechanical Properties of Polymers. *Biosurfaces* 2015.
- [2] C. E. Majewski, H. Zarrinhalam, N. Hopkinson. Effects of Degree of Particle Melt and crystallinity in SLS Nylon-12 parts.
- [3] C. Kummert and H.-J. Schmid. The Influence of Contour Scanning Parameters and Strategy on Selective Laser Sintering PA613 Build Part Properties.
- [4] Stéphane Dupin, Olivier Lame, Claire Barrès, and Jean-Yves Charneau. 2012. Microstructural origin of physical and mechanical properties of polyamide 12 processed by laser sintering. *European Polymer Journal* 48, 9, 1611–1621. DOI: <https://doi.org/10.1016/j.eurpolymj.2012.06.007>.
- [5] Thomas L. Starr, Timothy J. Gornet, and John S. Usher. 2011. The effect of process conditions on mechanical properties of laser-sintered nylon. *Rapid Prototyping Journal* 17, 6, 418–423. DOI: <https://doi.org/10.1108/13552541111184143>.
- [6] Thomas Stichel, Thomas Frick, Tobias Laumer, Felix Tenner, Tino Hausotte, Marion Merklein, and Michael Schmidt. 2017. A Round Robin study for Selective Laser Sintering of polyamide 12: Microstructural origin of the mechanical properties. *Optics & Laser Technology* 89, 31–40. DOI: <https://doi.org/10.1016/j.optlastec.2016.09.042>.
- [7] Andreas Wegner. 2015. *Theorie über die Fortführung von Aufschmelzvorgängen als Grundvoraussetzung für eine robuste Prozessführung beim Laser-Sintern von Thermoplasten*. Universität Duisburg-Essen, Duisburg-Essen.
- [8] Andreas Wegner and Gerd Witt. 2019. Adjustment of isotropic part properties in laser sintering based on adapted double laser exposure strategies. *Optics & Laser Technology* 109, 381–388. DOI: <https://doi.org/10.1016/j.optlastec.2018.08.017>.